PERSPECTIVE

Colloidal stability of the living cell

Håkan Wennerström[a,1], Eloy Vallina Estrada[b], Jens Danielsson[b], and Mikael Oliveberg[b,1]

Edited by Michael Levitt, Stanford University, Stanford, CA, and approved March 13, 2020 (received for review November 14, 2019)

Cellular function is generally depicted at the level of functional pathways and detailed structural mechanisms, based on the identification of specific protein–protein interactions. For an individual protein searching for its partner, however, the perspective is quite different: The functional task is challenged by a dense crowd of nonpartners obstructing the way. Adding to the challenge, there is little information about how to navigate the search, since the encountered surrounding is composed of protein surfaces that are predominantly "nonconserved" or, at least, highly variable across organisms. In this study, we demonstrate from a colloidal standpoint that such a blindfolded intracellular search is indeed favored and has more fundamental impact on the cellular organization than previously anticipated. Basically, the unique polyion composition of cellular systems renders the electrostatic interactions different from those in physiological buffer, leading to a situation where the protein net-charge density balances the attractive dispersion force and surface heterogeneity at close range. Inspection of naturally occurring proteomes and in-cell NMR data show further that the "nonconserved" protein surfaces are by no means passive but chemically biased to varying degree of net-negative repulsion across organisms. Finally, this electrostatic control explains how protein crowding is spontaneously maintained at a constant level through the intracellular osmotic pressure and leads to the prediction that the "extreme" in halophilic adaptation is not the ionic-liquid conditions per se but the evolutionary barrier of crossing its physicochemical boundaries.

cellular organization | protein–protein interactions | electrostatics | halophilic adaptation | ion screening

The exploration of cellular systems has so far been focused on the specific aspects of their function, typically in the form of ordered structures, molecular pathways, and patterns of genetic conservation (1). Even so, it is evident from the structures of existing protein–protein interactions that the specific interfaces only compose a minor fraction of the proteins' total surface areas (2). It is also clear that the residues occupying the surfaces outside these conserved binding sites vary substantially across divergent organisms (3). For proteins at work, this means that the most frequent interactions will be with the "nonconserved" background, and—from the perspective of maintaining specific pathways—this appears as a formidable challenge indeed (Fig. 1), especially since a successful search is required for cellular survival. Inspired by the stabilizing action of inert osmolytes, the main influence of intracellular crowding was initially thought to be passive and exerted through steric exclusion (4). However, this view has recently changed. Contrasting with the predictions from steric exclusion alone, the transfer of proteins into live cells leads sometimes to a distinct decrease in thermodynamic stability (5). The cause of this destabilization is attributed to so-called quinary interactions (6), adding preferential weak-interaction terms to the protein-folding equilibrium (5, 7). Interestingly, these quinary interactions also depend critically on the surface mutation and type of host cells (8, 9). In a systematic study of more than 130 mutations of three phylogenetically divergent proteins in *Escherichia coli*, the intracellular motions were found to correlate uniformly with the physicochemical properties of the "nonconserved" areas of the protein surfaces (10). Although the original versions of the human proteins were initially found to "stick" to the evolutionary foreign interior of the

[a]Division of Physical Chemistry, Department of Chemistry, Lund University, 22100 Lund, Sweden; and [b]Department of Biochemistry and Biophysics, Arrhenius Laboratories of Natural Sciences, Stockholm University, S-106 91 Stockholm, Sweden

Author contributions: H.W., J.D., and M.O. designed research; H.W., E.V.E., and M.O. performed research; H.W., J.D., and M.O. analyzed data; and H.W., E.V.E., J.D., and M.O. wrote the paper.

The authors declare no competing interest.

This article is a PNAS Direct Submission.

[1]To whom correspondence may be addressed. Email: hakan.wennerstrom@fkem1.lu.se or mikael.oliveberg@dbb.su.se.

This article contains supporting information online at https://www.pnas.org/lookup/suppl/doi:10.1073/pnas.1914599117/-/DCSupplemental.

First published April 13, 2020.

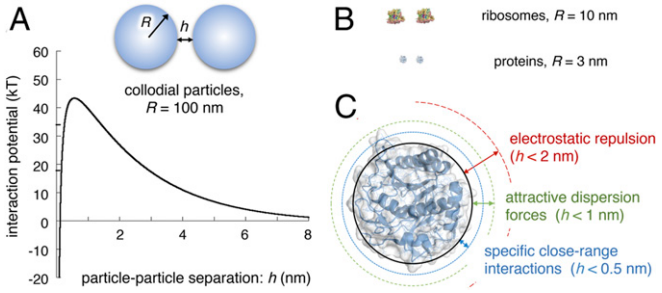

Fig. 1. Dimensions and forces of biological macromolecules. (*A*) Colloidal description of particles (R ≥ 100 nm) yielding kinetic stability through a high repulsive association barrier. (*B*) Relative sizes of ribosomes and proteins, constituting the dominant fraction of soluble cytoplasmic components. (*C*) The separation distance (*h*) regimes of the balancing forces that modulate protein–protein interactions in vivo.

E. coli host, they were easily brought back to normal diffusive motion by single, or a few, point mutations, rendering their surface properties more bacterial-like (10). The dominating factor here is the protein repulsive charge, followed by the electric-dipole moment and exposed surface hydrophobicity (10). Upon accounting for these surface quantities, the analyzed proteins define a common plane in the property space, irrespective of their evolutionary origin (10) (Fig. 2). The "nonconserved" protein surfaces are thus not passive but seem to actively control the background cross-talk through physicochemical cues coded by the genomes (6, 8, 10). Even though this "background" is not as strictly conserved as the specific cellular functions, it is nonetheless evident from natural proteomes that there is a consistent bias to negative surface-charge densities (11–14) (Fig. 2). This intriguing possibility calls now for detailed mechanistic elucidation. We target here the problem by presenting a colloidal description of the cellular system, based on the protein sizes, level of crowding, and ion composition of growing *E. coli* cells. The results show that, due to the excess negative charge of the *E. coli* proteins, the screening of the electrostatic forces is reduced, leading to a non-exponential scaling at physiologically relevant protein–protein separations. This promotes swift close-range sampling of the protein environment, avoiding the dispersion-force minima characteristic for larger colloidal particles (pp. 326–327 in ref. 15). The electrostatic correlations associated with these protein motions are also suggested to significantly contribute to the intracellular osmotic pressure, driving the system to self-organization with respect to protein–protein distances and physiological protein concentration. Finally, the key role of negative charge in maintaining proteome dispersion points to an evolutionary conundrum with implications for the ongoing discussion about "habitat-specific genomes" (16): How can evolution gradually cross the physicochemical barrier of nullified proteome repulsion at ∼1 M cytosolic salt, separating *Halobacteria* from other organisms?

Model Description, Data Support, and Unanswered Questions

Molecular Interactions and Criteria for Protein Dispersion in Live Cells. The functional organization of the cell is based on the interactions between its different intracellular species. Although these interactions show an amazing richness in detail, it is possible to identify the key mechanisms that account for the general features. At long range, the electrostatic force stands out as dominating, and at closer range this is complemented by the attractive dispersion force. At atomic contact, there is additionally a "sharp stop" due to the strong Pauli repulsion. This type of description is formally simple and underlies, for example, molecular dynamics simulations with explicit solvent molecules. Even so, it remains challenging to keep track of the interactions involving all of the solvent molecules in a more conceptual description. It is thus useful to make a coarse graining involving an average over the solvent degrees of freedom (17). Such averaging leads to a modified description of the interactions, which has the character of free energies. The dispersion attraction is still in place but the solvent averaging reduces its magnitude (*SI Appendix*). Moreover, the solvent averaging gives rise to the attractive, so-called hydrophobic, term, which typically exceeds the dispersion force at close range. The key difference is that the hydrophobic interaction is specific to apolar patches, whereas the dispersion force applies rather uniformly to all atoms, including those that are charged. Also, the free-energy character of the hydrophobic interaction

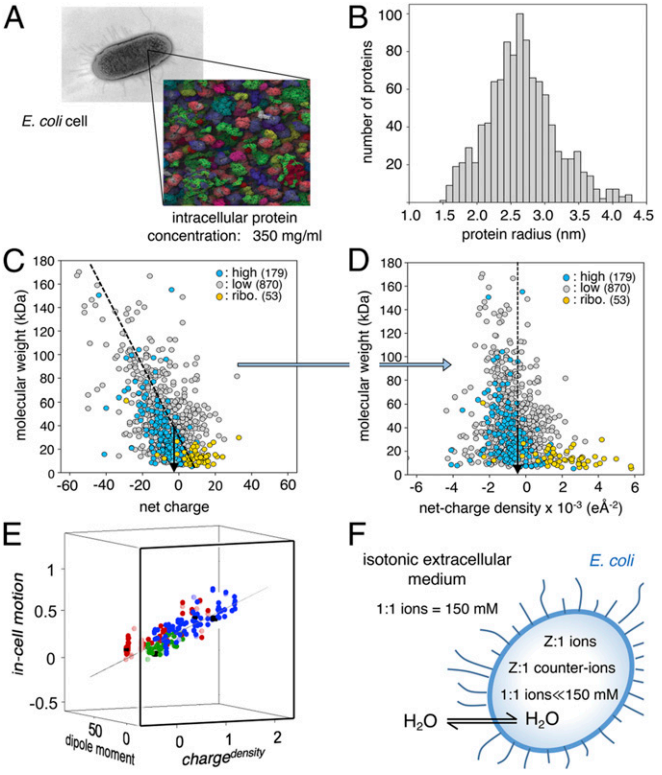

Fig. 2. Crowding, properties, and motions of proteins in *E. coli* cells. (*A*) It is kinetically favorable for the cell to be compact to ensure short diffusion paths, but not so compact that the diffusional motion becomes restricted. Judging by *E. coli*, the optimal balance is at protein concentrations around 350 mg/mL (25, 26). Crowding panel reprinted from ref. 27, which is licensed under CC BY 4.0. (*B*) Hydrodynamic radii of soluble proteins in *E. coli*. (*C*) Protein size shows a slanted correlation with net charge. (*D*) Upon rescaling to surface net-charge density, the distribution becomes approximately normal. (*E*) Normalized protein motion in the *E. coli* cytosol as measured by in-cell NMR rotation-correlation times. The projection is along the data plane and shows the dependence on negative net-charge density and the protein-dipole moment. Data include >130 surface mutations of three proteins: bacterial TTHA (blue), human HAH1 (red), and human SOD1-barrel (green). Panel adapted from ref. 10. (*F*) Differences in ion composition between the extracellular medium and the *E. coli* cytosol.

adds a distinct temperature dependence, which ultimately manifests in protein-cold unfolding (5).

To maintain the proteins dispersed, the attractive components need naturally to be neutralized or exceeded by repulsive ones, and in vivo the dominant repulsion is from the long-range interactions between net-charged species. At closer distances, there is also a repulsion from spatial restriction of surface flexibility, leading to a local decrease in configurational entropy (18). The range of this "entropic-cushioning" effect is here determined by the volume sampled by the flexible surface side chains (Fig. 1). A third repulsive mechanism at short range is the desolvation of polar groups facing an apolar surface, often described in terms of unmatched hydrogen bonds. With respect to particle–particle distance (h), the interaction between two proteins can thus be seen as having three regimes (Fig. 1). At distances larger than $h \approx$ 1 nm, the interaction is dominated by the charge–charge repulsion, below $h \approx 1$ nm the charge–charge repulsion becomes modified by the attractive dispersion force, and, finally, below $h \approx$ 0.5 nm the interaction is taken over by strong short-range components that can be either repulsive or attractive, depending on orientation. It is the latter short-range regime that ensures molecular specificity and biological function, as illustrated by numerous structures in the Protein Data Bank. Even so, the probability of establishing a specific interface depends not only on the close-range contacts but also on the long-range repulsion through the height of the association barrier. If the electrostatic repulsion is too weak, the proteome will rapidly get stuck in the close-range regime, and if it is too strong the encounters will become too rare. For an organism to properly function, the system should thus show marginal stability against association. The situation resembles that of first-order protein folding, where the conflicting requirements of high specificity and swift conformational search are satisfied through marginal protein stability (19). To quantitatively describe the intracellular interactions, we make use of the colloidal formalism (15, 20). Although this is more commonly used to describe dispersion of larger particles with radii >10 nm, we demonstrate that it can also be applied to crowded systems of proteins (Fig. 1). An analogy is the established colloidal description of micelles (21), the sizes and surface properties of which are similar to *E. coli* proteins (Fig. 2).

Size and Charge of Intracellular Proteins. We focus first on the proteome of *E. coli*, where there is validated information about intracellular conditions, expression levels, and intracellular protein behavior. Ishihama et al. (22) have produced abundance data for the cytosolic *E. coli* proteins, most of which are soluble and essentially globular. Of the 1,102 proteins identified, a subset of 179 nonribosomal proteins was denoted as highly abundant with copy number values above 2050. For each protein, we derived the molecular weight, hydrodynamic radius (R_p) according to Danielsson et al. (23), and solvent-accessible surface area assuming spherical shapes (*SI Appendix*). The results show that the size distribution of the nonribosomal proteins is centered around $R_p = 2.7 \pm 0.5$ nm, with a slight shift to $R_p = 2.5 \pm 0.5$ nm for the high-abundance subset (*SI Appendix*, Table S1 and Fig. 2). The latter is in full agreement with the value of $R_p = 2.5$ nm from https://bionumbers.hms.harvard.edu/search.aspx. Second, we calculated the protein net charge at pH 7.5 from the amino acid composition using model compound pK_A values (*SI Appendix*). Most notably, the majority of the soluble *E. coli* proteins are biased to net-negative charge (Fig. 2). The minority of proteins with positive net charge encompass, for example, the ribosomal proteins that bind to negatively charged RNA in vivo (24)(Fig. 2).

When it comes to the property under selective pressure, however, the skewed correlation between molecular weight and protein net charge indicates that there is more to it. Consistently, the plot straightens up into an overall symmetric distribution centered at −1e/11 nm^2 upon accounting for the differences in protein surface area, that is, by rescaling to net-charge density (*SI Appendix*, Table S1). There are two implications of this result. First, it indicates that there is a biological selection for net-charge density rather than net charge itself. Second, it supports our notion that *E. coli* can be modeled as a colloidal system, as the latter predicts scaling with net-charge density (discussed below). The value of −1e/11 nm^2 is also in the range of that of RNA in complex with positively charged proteins (i.e., ribosomes, DNA/chromatin, and DNA/repressor proteins in prokaryotes). The lipid part of membranes has a somewhat higher charge density in the range of −1e to −3e/11 nm^2, modified in vivo by the embedded membrane proteins. As controls, we calculated the protein dimensions and net-charge densities by a series of other methods and datasets, including X-ray structures, arriving at similar results (*SI Appendix*). These consistent features lend support to our treatment of the intracellular compartment as an aqueous environment with uniformly negative particles (Fig. 2).

Ion Composition and Electrostatic Screening of Intracellular Interactions. Since water diffuses relatively freely over the plasma membrane and inside the cell, the intracellular compartment obtains a uniform osmotic pressure set by the extracellular solution. For *E. coli*, like many other cells, the optimal value for this osmotic pressure matches that of 150 mM NaCl (28). In the 150 mM NaCl growth medium, the dominant contribution to the osmotic pressure is thus from the entropy of mixing of small 1:1 electrolytes (Na^+, Cl^-), yielding a Debye-screening length of $\lambda_D = 0.8$ nm (*SI Appendix*, Eq. **S13**). Simply speaking this number corresponds to the distance where charged particles start to "feel" one another. Inside the cells submerged in this medium, however, the situation turns out to be quite different (Fig. 2). The selectivity in ion transport across the plasma membrane means that ions inside and outside the cell need not to be in equilibrium. One finds mainly three types of charged species in the cytosol: small cations (Na^+, K^+, Mg^{2+}), small anions (Cl^-, HCO_3^-, $H_2PO_4^-$), and net-negative polyions of colloidal size (e.g., proteins, nucleic acids, and membranes). Depending on physiological status, there are also varying levels of organic anions like glutamate/acetate and small metabolites like ADP/ATP (29, 30). Cell-content analysis reveals that the concentration of small anions is kept notably low at 6 to 30 mM, while the concentration of small cations is much higher at 80 to 150 mM (31, 32). The reason for this mismatch is that the majority of negative charges are tied to macromolecules in the form of large polyanions. The proteins can here be denoted as Z:1-electrolytes, with Z between 5 and 10 (Fig. 2). Importantly, this intracellular bias of negative charge to proteins and other macromolecules has key implications for the electrostatic screening, which is rendered different from that in the isotonic extracellular medium. As an approximate value, the intracellular concentration of 20 mM 1:1-electrolyte yields a Debye screening length of 2.2 nm, compared to 0.8 nm in [NaCl] = 150 mM (*SI Appendix*, Eq. **S13**). The screening length inside the cell is thus considerably longer than in physiological buffer, making the proteins "feel" one another over larger distances. From an electrostatic perspective, the intracellular medium cell is thus different

from the [NaCl] = 150 mM solution, and the in-cell interactions are not adequately described by potentials with a screening length of 0.8 nm. Likewise, the electrostatic contribution to enzyme activities and conformational equilibria are also bound to be different from those in physiological saline because the residue pK_A values often found to influence these processes rely on the detailed electrostatic environment, as exemplified by the sometimes very complex pH and ionic strength dependence of enzymatic turnover (33). From an experimental perspective, this means that it is nontrivial to select an in vitro medium that accurately represents the in vivo electrostatic conditions. A prudent approach is thus to vary the salt content over a reasonable range to monitor the effects and to consider this response upon translation to in vivo behavior.

Quantitative Description of the Intracellular Protein–Protein Interactions. Protein–protein interactions are typically treated as ideal two-particle systems with an emphasis on the short-range specific features. In the crowded cells, however, such simplified descriptions are not valid, since each protein interacts simultaneously with several others. This requires the introduction of many-body corrections. We recently addressed this problem by developing an approximate description of the electrostatic interactions in concentrated systems of charged colloidal spheres (34). An essential feature of this formalism is that in crowded systems, where surface-to-surface separations are smaller than the particle radii, one can apply the simplifying Derjaguin approximation (35). Here we extend this idea to describe the diffusive protein–protein interactions in crowded *E. coli* cells. As a basis for our calculations we use the *E. coli* proteome characteristics (Fig. 2), a protein content of 35% V/V and a Debye screening length of 2.2 nm (discussed above). Moreover, we describe the proteins as charged spheres with a uniform radius of 2.5 nm, matching the high-abundance average (*SI Appendix*). For a start, the negative repulsive charge will result in positional correlations, since the proteins tend to avoid one another. This has the consequence that there is an optimal center to center separation r_{opt} (Fig. 3), which decreases as the protein concentration (c_p) increases:

$$r_{opt} \propto c_p^{-1/3}. \quad [1]$$

For uniform spheres, close packing occurs at a volume fraction of 74% and, by a scaling argument, the optimal center-to-center distance at 35% (V/V) is $r_{opt} = 2(74/35)^{1/3} \approx 2.57R_p$. With $R_p = 2.5$ nm, the corresponding surface to surface separation is $h = 0.57 \cdot R_p = 1.4$ nm, which is smaller than the electrostatic screening length (Fig. 3). Despite the proteins only feeling repulsive interactions, there is a local potential minimum at r_{opt}. Knowing both the protein charge and concentration, we first address the conditions around the optimal position r_{opt}. The nature of the local potential well [V_{eff} (z)] is estimated by assuming that the central protein is on average symmetrically surrounded by n neighbors, each of which interacts through a pair potential (V_p). The local potential is to second order in the displacement-coordinate z (34) according to

$$V_{eff}(z) = \frac{n}{6}\left\{\frac{d^2V_p}{dr^2}(r_{opt})\right\}z^2, \quad [2]$$

where V_p has contributions from both the electrostatic and the dispersion interaction. The electrostatic part can be estimated

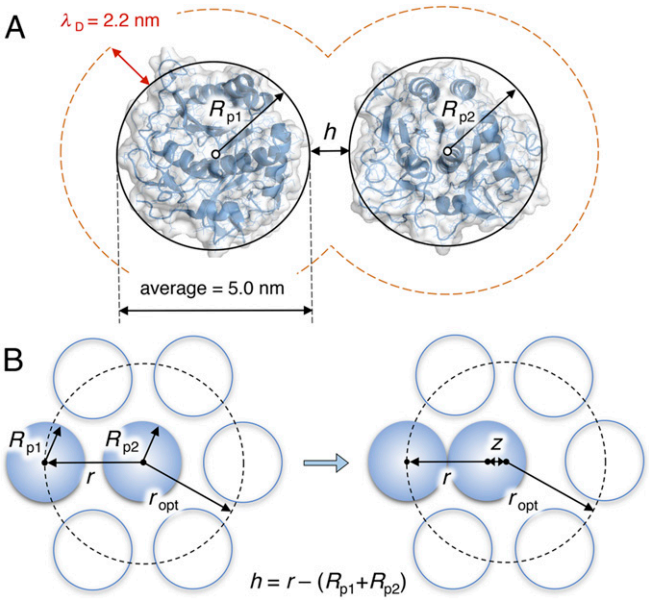

Fig. 3. Description of intracellular protein–protein interactions. (*A*) Dimensions of typical *E. coli* proteins, where the effective Debye screening length (λ_D) exceeds the protein–protein separation (h). (*B*) Schematic single layer ($n = 7$) of the interaction network, outlining the spatial parameters of *SI Appendix* and Eqs. 1–5. The resulting interaction potential for *E. coli* proteins is shown in Fig. 4.

by noting that $h \approx R_p/2$ (Fig. 3). We can then use the Derjaguin approximation (35) and the asymptotic form of the interaction between two charged planes (15) to obtain the electrostatic contribution (*SI Appendix*):

$$F_{el}(h) = -\frac{dV_p^{el}}{dh} = -128\pi kT\frac{R_{p1}R_{p2}}{(R_{p1}+R_{p2})}c_e\lambda_D\Gamma_0^2e^{(-h/\lambda_D)}; \quad \frac{d^2V_p^{el}}{dh^2} = \frac{dF_{el}(h)}{dh}, \quad [3]$$

where c_e is the1:1-electrolyte concentration and Γ_0 is a dimensionless parameter determined by c_e and surface-charge density (chap. 3 in ref. 20).

Regarding the dispersion attraction, this varies as r^{-7} for proteins at separations larger than their radii ($r >> 2R_p$), making it negligible at larger distances. At the separations relevant in vivo, however, the effective distance dependence is significantly changed as each molecular segment of a protein provides its own r^{-7} contribution to the net force. For geometrical reasons, this causes the net force to depend progressively less strongly on separation as r decreases. Another property of the dispersion force is that it is proportional to the product of the protein volumes at large separations, while it scales with the mean-protein radius at small separations. In this limit, the general expression for the dispersion force reduces to (15)

$$F_{disp}(h) = -\frac{R_{p1}R_{p2}}{6(R_{p1}+R_{p2})}H_{pwp}\frac{1}{h^2}, \quad [4]$$

where $h = r - (R_{p1} + R_{p2})$ and H_{pwp} denotes the dispersion part of the Hamaker constant for interaction across aqueous medium (p. 266 in ref. 15). As described in *SI Appendix*, we can then obtain explicit expressions for both the electrostatic and dispersion contributions to the effective potential $V_{eff}(z)$ in Eq. **2**.

With estimates of the parameters from the high-abundance dataset, that is, $R_{p1} = R_{p2} = 2.5$ nm and a net-charge density of –0.09 e/nm^2, we find an electrostatic contribution of 1.83×10^{-4}J/m^2 balanced by a dispersion part of -4.3×10^{-4}J/m^2. With $n = 8$ we obtain

$$V_{\text{eff}}(z) \approx 1.9 \times 10^{-3} z^2 \left(\text{J/m}^2\right). \quad [5]$$

Two qualitatively important conclusions follow from this potential estimate. First, it explicitly shows that the electrostatic repulsion dominates the dispersion attraction at average separations. Second, the effective local repulsion is weak enough to allow swift surface probing by local thermal motions (i.e., the potential is <kT for relevant displacements).

Implications for the Crowded* E. coli *Interior. To ensure cellular function, the proteins need not only to be suitably dispersed but must also be allowed to come in close-enough contact to reversibly search for specific short-range interactions (36). In this search regime ($h << R_p$), the electrostatic and the dispersion terms are both dominated by the direct pair interaction, and the restoring force from other neighbors is small. The magnitude of the electrostatic force (Eq. **3**) depends here on the protein surface-charge density, rather than on the global net charge, explaining the experimentally observed in-cell mobility behavior (Fig. 2). We also note from Eqs. **2** and **3** that the electrostatic and dispersion forces are both proportional to $R_{p1}R_{p2}/(R_{p1} + R_{p2})$, rendering their relative magnitudes independent of protein size at close range. Taken together, these findings provide a functional rationale for an evolutionary preferred surface-charge density in naturally occurring proteomes (Fig. 2).

Even though the $1/h^2$ divergence of the dispersion attraction (Eq. **4**) becomes eliminated by the atomic-nature contributions at close range, it can still promote aggregation at the isoelectric point, as is well known in protein purification. At physiological pH, however, the negative surface-charge density adds a compensating repulsion. This repulsion not only dominates at long range but is also strong enough to weaken the dispersion attraction at short range where the specific surface interactions come into play. In the regime where only counter ions occupy the interaction gap, the electrostatic contribution changes from an exponential to an algebraic distance dependence and diverges as $1/h$ (32). As with the $1/h^2$ divergence of the dispersion attraction, this $1/h$ divergence is eliminated at separations where the discrete atomic nature of the charges becomes influential. The competition between these generic attractive and repulsive components is quantified in Fig. 4, showing the calculated interaction potential between two proteins of radius 2.5 nm (*SI Appendix*). In essence, the force cancellation yields a generic weakly repulsive force down to separations of around 0.5 nm, well-suited for being sampled by physiological thermal fluctuations (Fig. 4). The *E. coli* proteome seems thus to represent a system at thermal equilibrium with respect to association degrees of freedom. This equilibrium situation is analogous to what is found in vitro for micelles (21) but different from the kinetic stability of conventional large-particle colloids (chap. 8 in ref. 20) (Fig. 1). In the latter case, the barrier for irreversible association can be >30 kT, maintaining long-time solubility. The corresponding barrier for the average *E. coli* protein is here calculated to just ~2 kT but can still yield solubility for indefinite time if the short-separation well is not too deep (Fig. 4). From a biological perspective, this situation makes perfect sense: The proteome is not only optimized for solubility but also for reversible close-range search. Regarding specific recognition, the force cancellation extends all of the way into the regime where the chemical ruggedness of the protein surfaces becomes dominant (Fig. 4). As such, the association potential seems tuned by net-charge density to facilitate the dynamic probing of specific surface details, without getting trapped like larger colloidal particles (15) (Fig. 1). Drawing a parallel to real bacteria, Cayley et al. (26) and Cayley and Record (37) observe effects on the *E. coli* function upon perturbing the intracellular 1:1-salt concentration that are persuasively explained by the present results. Essentially, the *E. coli* growth is mitigated under conditions where the intracellular charge repulsion deviates from normal and, to maintain low intracellular-charge screening in growth medium with [NaCl] >150 mM, the cells need to resort to energy-consuming import of compatible osmolytes (*SI Appendix*). These studies thus bring focus on the generic coupling between the intracellular composition and the external-osmotic pressure, as discussed next.

Contributions to the Intracellular Osmotic Pressure. Examples of how osmotic perturbations disturb cellular function is found in traditional food preservation, that is, freezing, drying, and adding

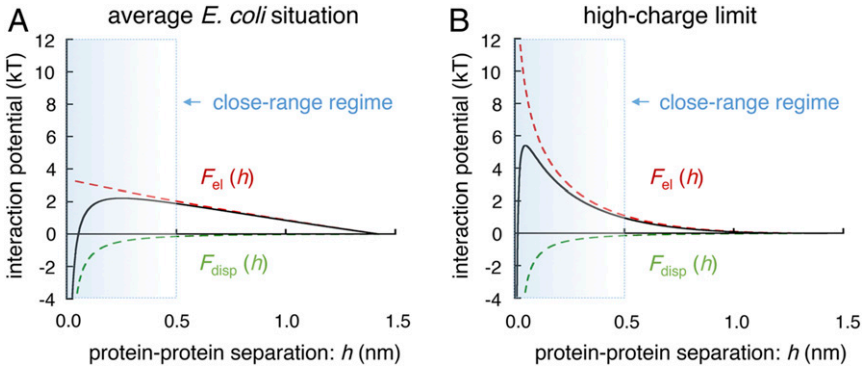

Fig. 4. Intracellular interaction potential calculated from the average characteristics of the *E. coli* proteome (*SI Appendix*). (*A*) The interaction potential of the *E. coli* proteins calculated from the asymptotic form in Eq. 3, valid for intermediate and longer range. (*B*) Corresponding potential at the high-charge limit, exemplifying the increased repulsion at short range between proteins at the extreme negative side of the *E. coli* net-charge density distribution (Fig. 2). In both cases, the proteins lack the deep association minima and large kinetic barriers of larger colloidal particles, suggesting that the protein–protein encounters are maintained at thermodynamic equilibrium (cf. Fig. 1).

salt or sugar (38). The increased osmotic pressure achieved by these methods extracts the intracellular water from any contained microbes, collapsing their cytosolic components and terminating growth. Normally, the extracellular osmotic pressure of *E. coli* is determined by the entropy of mixing of small 1:1-electrolytes like Na^+ and Cl^- ions, with an optimal concentration around 150 mM. Given that the intracellular salt concentration is still lower than that of the preferred growth medium, this raises the question of how the cells generate the cytosolic osmotic pressure. The estimated 20 mM 1:1-electrolyte is clearly not enough on its own (Fig. 2). Additionally, the proteins at a concentration of ∼10 mM and an average net charge of Z = −8 (*SI Appendix*, Table S1) will provide ∼80 mM monovalent counter cations, plus a similar number from the nucleic acids and charged lipids. Since these counter cations are attracted to the larger negatively charged polyanions, however, their osmotic contribution is reduced relative to that under ideal mixing conditions. Our estimate is thus that the total contribution of small ions to cellular osmotic pressure equals less than [NaCl] = 85 mM = 170 mOsm (chap.14 in ref. 15). As outlined in *SI Appendix*, the *E. coli* cells also recruit electrically neutral osmolytes to balance the osmotic pressure under high-salt stress, but under optimal growth conditions the levels of these molecules are negligible (37). Finally, *E. coli* maintains a turgor pressure of ∼1 bar across the cell membrane in 150 mM growth medium (39). This internal pressure translates to an intracellular excess of 20 mM 1:1-electrolyte, increasing the physiological osmotic-pressure equivalent from 150 to 170 mM NaCl = 340 mOsm. A conservative estimate is then that the combined contribution of small electrolytes and osmolytes to the cellular osmotic pressure is less than 50%. We point here to the possibility that the missing component stems from the proteins themselves. The argument is as follows. Because the proteins electrostatically repel one another, their translational degree of freedom gets more and more confined the higher the concentration. As is well known for hard-sphere systems, this leads to a positive deviation from the translational entropy obtained from the ideal mixing approximation (40). At a crowding level of 35% V/V, the translational degrees of freedom contribute a factor of 5 more than the ideal mixing case, and in this regime the nonideality depends strongly on both concentration and the nature of the protein–protein interactions. This repulsion-induced decrease in translational entropy will naturally lessen upon expansion of the cell, giving an intrinsic contribution to the osmotic pressure. In contrast to the hard-sphere systems, the protein–protein interactions are also orientation-dependent and controlled by the protein surface details (Figs. 1 and 2). Upon cellular expansion, the orientational correlations will also lessen, leading to gain in rotational entropy and an additional contribution to the osmotic pressure. Considering the sensitivity of these nonideal factors to the surface heterogeneity and precise cellular composition, it is yet difficult to quantitatively estimate their impact. Even so, it seems clear that the chemical characteristics of the protein surfaces themselves have a significant influence on the cytosolic-osmotic pressure through their coupling to the system's translational and rotational entropy. It also follows that this influence can be under selective control through optimization of the protein-surface details.

The Divergent Adaptation of Halophilic Archaea. The generic role of charge in maintaining protein dispersion is ultimately manifested by the salt-thriving *Halobacteria*. The adaptation of these organisms to saturated-salt biotopes has led to the curious development of similarly salty cytosols to mitigate osmotic-pressure problems (11). As an apparent compensation for the loss of net-charge repulsion, their proteomes have evolved net-charge densities that are 10 times more negative than in *E. coli* (Fig. 5 and *SI Appendix*, Fig. S5). Thus, from a physicochemical standpoint, these extremophiles have found a way to support the fundamental biochemical processes in a solvent that can be described as an ionic liquid. Hydrophobic, or more precisely solvophobic, interactions are still operative under these conditions, although it is the cohesion of the ionic species rather than the water that promotes the effect (41). The same is true for the attractive dispersion force and the repulsion mechanism due to restricted freedom of surface groups. Regarding the electrostatics, however, the conventional electrical double-layer repulsion is virtually absent as the formal Debye length at multimolar 1:1 ions is smaller than an atom size. Nonetheless, it is found that for ionic liquids and highly concentrated electrolytes there is still a measurable repulsion between similarly charged surfaces (42–44). The conventional Debye screening is quenched and replaced by weaker screening with much larger decay length due to the strong ion–ion correlations (45, 46). Most notably, the consequence of this high-salt effect is a nonmonotonic variation of the screening length with electrolyte content (47). Below 0.5 M, the charge repulsion follows conventional Debye decay, between 0.5 and 1.5 M it is effectively absent, and above 1.5 M the charge repulsion restores to become effective again (Fig. 5 and *SI Appendix*). We denote tentatively these bounds as the "Debye," "eclipse," and "ionic-liquid" regimes, respectively. From the arguments above, it is thus expected that an organism more easily adapts to the Debye and ionic-liquid regimes than to the eclipse regime, since the latter does not allow for intracellular tuning by charge repulsion. There may indeed be other ways to deal with the situation of excessively short screening lengths, but the constraints are likely challenging. An interesting detail is also that *Halobacteria*, where the osmotic contribution from the high internal [salt] is bound to override that from the proteins, are unique by lacking cellular turgor pressure (11).

In line with this conjecture, existing proteomes show a distinctly partitioned distribution of net-charge densities (Fig. 5). At the far negative end are the *Halobacteria* with ionic-liquid cytosols and to the right are the majority of other organisms with "typical" cytosols. Between the *Halobacteria* and the other organisms there

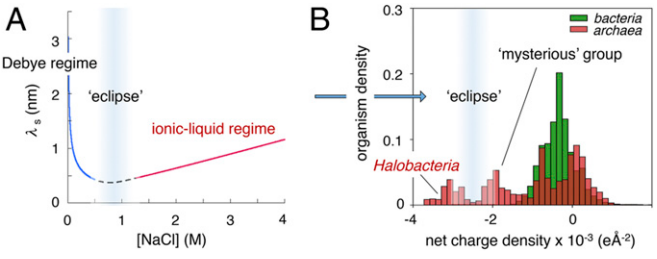

Fig. 5. Minimum of effective screening length (λ_s) yields an electrostatic "eclipse" around [NaCl] = 1 M. (*A*) Up to ∼[NaCl] = 1 M, the screening length follows conventional Debye–Hückel decline, whereas in the ionic-liquid regime it restores due to ion–ion correlations (44, 46). Between these limits is an "eclipse" where the electrostatic interactions are severely mitigated at λ_s < 0.5 nm. (*B*) Since long- and medium-range charge interactions seem crucial for cellular function, intracellular salt concentrations around the electrostatic "eclipse" are expected to be most unfavorable. Correspondingly, there is a minimum in the distribution of proteome net-charge densities separating *Halobacteria* from other organisms.

is a gap (Fig. 5). Since the *Halobacteria* are so far the only organisms with established ionic-liquid interior, it is tempting to assume that this gap coincides with the unfavorable eclipse regime. Although the trend remains qualitative until the detailed relation between intracellular salt and net-charge density is determined, we take this to underline that electrostatic repulsion of sizable range is indeed the favored mechanism for preventing general aggregation in vivo (48).

General Implications and Outlook

Long-Range Electrostatic Repulsion Is an Essential Organizational Principle. Although life is basically a chemical process, its very complexity at the cellular level is often taken to preclude basic atomistic description. In the present paper, we attempt to see how far this is true. Our starting point is the observation that the cytosolic *E. coli* proteome shows a uniform net-charge density of around $-1e/11\ nm^2$ (Fig. 2). From first principles, such excess charge provides a generic intermolecular repulsion that aids dispersion under crowded conditions. Since the nucleic acids and membranes carry similar or higher net-charge densities, we further conclude that this macromolecular dispersion reflects a physiological optimization. Even if the protein net-charge density distribution in Fig. 2 is broad and even spans over positive values, it does not falsify the idea of a functional charge bias. As mechanistic proof of principle, in-cell NMR analysis demonstrates that a mutational decrease of repulsive surface charge causes cytosolic proteins to "stick" to the *E. coli* interior, while a corresponding increase makes them less restricted (10). From the fact that a substantial fraction of the intracellular negative charge is permanently fixed to cytosolic proteins in the form of Z:1-polyions (Fig. 2), it is also evident that the physiological setting is chemically different from that in standard [NaCl] = 150 mM buffer where all anions are small and free to diffuse independently. A key consequence of this situation is that the charge–charge interactions will operate over longer distances in the cell than in [NaCl] = 150 mM buffer, simply because of mitigated small-ion screening (Fig. 2). Considering that many physiological processes are indeed controlled by biomolecular charge (49), this higher in vivo sensitivity to the electrostatic interplay is functionally reasonable. For example, when *E. coli* cells under conditions of hyperosmotic stress are forced to increase the cytosolic-charge screening by import of small salts, it comes with the cost of halted growth (50).

Notes on Biological Selectivity at Close Range. From the central dogma, biological function is optimized through natural selection at the level of amino acid composition. However, the universally present dispersion force, which may be the most significant attractive interaction in the cellular system, is not amenable to such selection because it shows little dependence on side-chain identity. Therefore, life has had to resort to other means. In a classical colloidal system, the particles are protected from aggregation by a large charge-repulsion barrier that kinetically deflects the particles from entering the attractive dispersion minimum (Fig. 1). Once they do, the particles are bound to be stuck. Such kinetic stability is clearly not appropriate for protein function. Nature's solution, it appears, is a tuning of the protein-charge repulsion (10, 11, 48) to a level where it just cancels the dispersion minimum at intermediate range, allowing swift dynamic encounters at close range (Fig. 4). The beauty of this optimization is that it "overrides" the unspecific character of the dispersion force by guiding the proteins directly into the regime where the highly selective amino acid details take over. As such, the in vivo protein dispersion can also be said to be at thermodynamic equilibrium, thus contrasting the kinetic stability of the typical colloidal system (Fig. 1). It further is evident that natural protein–protein interfaces depend critically on the complementary side-chain details, where any Brownian surface diffusion will cause substantial modulation of the close-range interactions as depicted in Fig. 4. Despite this microscopic complexity, we find it still useful to comment on the range and likely cellular impact of these close-range interactions. In doing so, we first emphasize that the potential derived from Eqs. **3** and **4** remains operative in this close-range regime, and that the various anisotropic contributions come in as additive terms with their own characteristic distance dependence. The first term to materialize is that from global protein dipoles, experiencing a shorter screening length than global net charge, and in the present case ~1 nm (51). At 1-nm separation, the basal potential in Fig. 4 thus gains an additional dipole component that is either repulsive or attractive depending on protein orientation. Naturally, this component will favor orientations where the dipoles are attractively aligned and contribute to "electrostatic steering" in the early association process (52). In terms of strength, the protein rotation-correlation times in *E. coli* display a significant and approximately linear dependence on the protein-dipole moment (10) (Fig. 2). At still shorter range are the contributions from higher dipole moments and point charges, which operate at distances matching their spatial separations on the protein surfaces, on average 0.59 nm for the *E. coli* proteins (*SI Appendix*, Table S4) (53). Like the dipoles, these interactions will contribute to interface steering (36), but at distances where also repulsive surface-entropy loss and other, more "glassy," contact terms start to kick in. Hence, if the net-charge repulsion is too small, the binding potential will bias the system closer to the glassy regime, arrest the dynamics, and cause the proteins to stick. Conversely, if the net-charge repulsion is too high, the close-range sampling may be lost altogether or mitigated to the extent that only the strongest binding sites remain attractive. Although the latter scenario promotes selectivity, it has the drawback of reducing binding probability. The analogous argument applies to the protein-search kinetics, based on the observation that exploratory surface diffusion is a key component of finding specific-binding fit (36): If the close-range search is too swift, the likelihood of finding the right binding partner is minimal and, if it is too long-lived, the proteins end up wasting time exploring nonpartners. As the majority of in-cell encounters are indeed bound to be unproductive, the latter situation must be avoided (10).

Regulation of the Physiological Osmotic Pressure. Under conditions where a cell neither swells nor shrinks its osmotic pressure matches that of the environment, that is, $\Pi_{cell} + P_{turgor} = \Pi_{buffer}$ (39). As outlined in Fig. 2, however, the source to the osmotic pressure is bound to be different on either side of the plasma membrane. Although this difference may be of little practical importance in the laboratory, it turns out to have implications for the mechanism of cellular self-organization. Under steady-state conditions, the *E. coli* content is constantly turned over by numerous metabolic processes: New molecules are synthesized, others are degraded, and there is import and export across the membrane (37). As these processes regulate the number of cytosolic molecules, they inherently regulate the osmotic pressure. This means that the osmotic pressure provides a thermodynamic coupling between all metabolic reactions adjusting the number of cytosolic molecules. Since the proteins, because of their correlated

charge interactions, contribute more per molecule to the osmotic pressure than the smaller solutes, it follows that their concentration is to some extent self-regulated. As an illustration, we imagine that we remove some proteins from the *E. coli* cytosol and replace them with the same volume of pure water. The remaining proteins will then naturally diffuse into the unoccupied volume and end up less concentrated. The decreased osmotic pressure accompanying this protein dilution will now force an efflux of cytosolic water, shrinking the cell until the cytosolic osmotic pressure has come to match that of the extracellular medium. This happens first when the original protein concentration and charge interactions are restored. Removing proteins will thus make the cell smaller and, vice versa, adding more proteins will make it larger.

Adaptation Across Marine and Freshwater Environments. Marine organisms are generally subjected to salt concentrations three times higher than that of physiological saline, that is, ~[NaCl] = 0.5M = 1 osmol. To avoid overcrowding and cellular collapse, the proteins and the 1:1-electrolytes cannot balance this osmotic pressure on their own but need help from synthesis or import of noncharged osmolytes (54). Even if this strategy is the norm in marine environments, it comes with a metabolic cost (54). The contrasting situation is found in fresh water with an osmotic pressure below 0.1 osmol. To match this environment, the proteins and their counterions need to dilute, but with the functional penalty of longer diffusion paths and increased protein–protein repulsion. Although cells can build up turgor pressures to reduce this effect, there is a limit in the mechanical stability of the outer membrane. Consistently, gram-positive bacteria that can sustain turgor pressures of ~20 bar = 0.8 osmol (55) are much more common in fresh water than in the sea (13). Freshwater cyanobacteria show moreover much higher turgor pressure than their halophilic relatives, where the latter takes advantage of the situation by resorting to thinner cell walls (56). The trade-off indicates that the high-turgor situation in fresh water is structurally costly and cannot easily be avoided by other means. Our osmotic pressure-centric reasoning ties thus in with the notion that adaptation of microorganisms across the marine and freshwater environments is an unusual and evolutionary demanding process (13, 57). Reflecting this osmotic challenge, the proteomes of marine-, brackish-, and freshwater-adapted bacteria show also a stepwise decrease in net-negative charge (13, 14). Although these conjectures remain speculative, the idea is out to be challenged. Whatever the answer may be, it seems likely that the osmotic pressure, through its thermodynamic coupling to charge repulsion and protein–protein separation, plays a more central physiological role than previously appreciated.

Halophilic Archaea. The generic role of macroscopic charge in maintaining intracellular dispersion is ultimately exemplified by the salt-thriving *Halobacteria* with ionic-liquid interiors and protein net-charge densities 10 times more negative than in *E. coli* (11) (Fig. 5). Given that the formal Debye length is negligible already at 1 M KCl, speculations have been that the role of the excessive protein charge in *Halobacteria* is not in repulsion per se but in increasing solubility by other means, for example through enhanced surface hydration (58) and specific-ion coordination (59). We question here the necessity of such additional mechanisms by pointing back to the generic electrostatics. The principal evidence is that, at sufficiently high salt concentrations, the electrostatic interactions are reestablished through ionic correlations (43, 45) (Fig. 5). With respect to the halophilic adaptation, however, this separation of the electrostatic influence into a low- and high-salt regime comes also with a twist: How does a cell evolutionarily cross the "eclipse" where the electrostatic interactions are bound to be inoperative? If selection cannot easily move from one solvent condition to the other, this will yield a barrier that isolates *Halobacteria* from other organisms. The existence of such a selective barrier is indeed indicated by a distinct gap in the distribution of net-charge densities across the various prokaryote species (Fig. 5). Although this idea needs further investigation, it is interesting to note that the very influence of net-charge repulsion on natural selection adds chemical rationale to the definition of "habitat genomes" (16, 60). How evolution may still surmount the electrostatic-depletion barrier seems best answered by the organisms closest to the "eclipse" regime (Fig. 5). Obvious candidates are the *Halobacteria* with least negative proteomes and the distinct but yet "mysterious" group of archaea at the negative side of the distribution of "typical" organisms (61). As discussed above, the general strategy for prokaryotes to handle variations in salinity seems to be the energy-consuming recruitment of compatible solutes (62), but how these stress molecules act to solubilize proteomes under conditions of diminished net-charge repulsion remains poorly understood (63). Adding to the challenge, the physiological levels of the small anions that are key to the intracellular screening remain notoriously difficult to determine (62). To stimulate further exploration of these fundamental aspects of cellular function, we fuel here the discussion by arguing that the most "extreme" in halophilic adaptation lies not in the biotopes themselves but rather in the evolutionary crossing of their chemical boundaries. After all, a halophile that survives in isolated brine pockets of geologically intact salt crystals (64) cannot be said to struggle with its environment: To some organisms, ionic-liquids are in fact as "physiological" as 150 mM NaCl.

Data Availability. Datasets and protocols are described in *SI Appendix*, and raw data are available from mikael@dbb.su.se.

Acknowledgments

This work was supported by Knut & Alice Wallenberg Foundation grant 2017-0041 and Swedish Research Council grant 2017-01517.

1 D. L. Nelson, M. M. Cox, A. L. Lehninger, *Lehninger Principles of Biochemistry* (Macmillan, 2017).
2 W. S. Valdar, J. M. Thornton, Protein-protein interfaces: Analysis of amino acid conservation in homodimers. *Proteins* **42**, 108–124 (2001).
3 B. Ma, T. Elkayam, H. Wolfson, R. Nussinov, Protein-protein interactions: Structurally conserved residues distinguish between binding sites and exposed protein surfaces. *Proc. Natl. Acad. Sci. U.S.A.* **100**, 5772–5777 (2003).
4 R. J. Ellis, Macromolecular crowding: Obvious but underappreciated. *Trends Biochem. Sci.* **26**, 597–604 (2001).
5 J. Danielsson *et al.*, Thermodynamics of protein destabilization in live cells. *Proc. Natl. Acad. Sci. U.S.A.* **112**, 12402–12407 (2015).
6 R. D. Cohen, G. J. Pielak, A cell is more than the sum of its (dilute) parts: A brief history of quinary structure. *Protein Sci.* **26**, 403–413 (2017).
7 A. C. Miklos, M. Sarkar, Y. Wang, G. J. Pielak, Protein crowding tunes protein stability. *J. Am. Chem. Soc.* **133**, 7116–7120 (2011).
8 L. Barbieri, E. Luchinat, L. Banci, Protein interaction patterns in different cellular environments are revealed by in-cell NMR. *Sci. Rep.* **5**, 14456 (2015).
9 S. Majumder *et al.*, Probing protein quinary interactions by in-cell nuclear magnetic resonance spectroscopy. *Biochemistry* **54**, 2727–2738 (2015).
10 X. Mu *et al.*, Physicochemical code for quinary protein interactions in *Escherichia coli*. *Proc. Natl. Acad. Sci. U.S.A.* **114**, E4556–E4563 (2017).

11 N. Gunde-Cimerman, A. Plemenitaš, A. Oren, Strategies of adaptation of microorganisms of the three domains of life to high salt concentrations. *FEMS Microbiol. Rev.* **42**, 353–375 (2018).
12 L. Koçillari, P. Fariselli, A. Trovato, F. Seno, A. Maritan, Signature of Pareto optimization in the Escherichia coli proteome. *Sci. Rep.* **8**, 9141 (2018).
13 P. J. Cabello-Yeves, F. Rodriguez-Valera, Marine-freshwater prokaryotic transitions require extensive changes in the predicted proteome. *Microbiome* **7**, 117 (2019).
14 J. Kiraga *et al.*, The relationships between the isoelectric point and: Length of proteins, taxonomy and ecology of organisms. *BMC Genomics* **8**, 163 (2007).
15 J. N. Israelachvili, "Electrostatic forces between surfaces in liquids: The electric "double-layer"" in *Intermolecular and Surface Forces* (Academic Press, ed. 3, 2015).
16 F. Dini-Andreote, F. D. Andreote, W. L. Araújo, J. T. Trevors, J. D. van Elsas, Bacterial genomes: Habitat specificity and uncharted organisms. *Microb. Ecol.* **64**, 1–7 (2012).
17 L. R. Pratt, M. I. Chaudhari, S. B. Rempe, Statistical analyses of hydrophobic interactions: A mini-review. *J. Phys. Chem. B* **120**, 6455–6460 (2016).
18 J. N. Israelachvili, H. Wennerstroem, Entropic forces between amphiphilic surfaces in liquids. *J. Phys. Chem.* **96**, 520–531 (1992).
19 M. Oliveberg, P. G. Wolynes, The experimental survey of protein-folding energy landscapes. *Q. Rev. Biophys.* **38**, 245–288 (2005).
20 D. F. Evans, H. Wennerström, *The Colloidal Domain: Where Physics, Chemistry, Biology, and Technology Meet* (Wiley, ed. 2, 1999).
21 H. Wennerström, B. Lindman, Micelles. Physical chemistry of surfactant association. *Phys. Rep.* **52**, 1–86 (1979).
22 Y. Ishihama *et al.*, Protein abundance profiling of the Escherichia coli cytosol. *BMC Genomics* **9**, 102 (2008).
23 J. Danielsson, J. Jarvet, P. Damberg, A. Gräslund, Translational diffusion measured by PFG-NMR on full length and fragments of the Alzheimer Aβ(1–40) peptide. Determination of hydrodynamic radii of random coil peptides of varying length. *Magn. Reson. Chem.* **40**, S89–S97 (2002).
24 S. Ahmad, A. Sarai, Analysis of electric moments of RNA-binding proteins: Implications for mechanism and prediction. *BMC Struct. Biol.* **11**, 8 (2011).
25 S. B. Zimmerman, S. O. Trach, Estimation of macromolecule concentrations and excluded volume effects for the cytoplasm of Escherichia coli. *J. Mol. Biol.* **222**, 599–620 (1991).
26 S. Cayley, B. A. Lewis, H. J. Guttman, M. T. Record, Jr, Characterization of the cytoplasm of Escherichia coli K-12 as a function of external osmolarity. Implications for protein-DNA interactions in vivo. *J. Mol. Biol.* **222**, 281–300 (1991).
27 S. R. McGuffee, A. H. Elcock, Diffusion, crowding & protein stability in a dynamic molecular model of the bacterial cytoplasm. *PLOS Comput. Biol.* **6**, e1000694 (2010).
28 M. T. Record, Jr, E. S. Courtenay, S. Cayley, H. J. Guttman, Biophysical compensation mechanisms buffering E. coli protein-nucleic acid interactions against changing environments. *Trends Biochem. Sci.* **23**, 190–194 (1998).
29 C. Feehily, K. A. Karatzas, Role of glutamate metabolism in bacterial responses towards acid and other stresses. *J. Appl. Microbiol.* **114**, 11–24 (2013).
30 B. Enjalbert, P. Millard, M. Dinclaux, J. C. Portais, F. Létisse, Acetate fluxes in Escherichia coli are determined by the thermodynamic control of the Pta-AckA pathway. *Sci. Rep.* **7**, 42135 (2017).
31 S. Sundararaj *et al.*, The CyberCell database (CCDB): A comprehensive, self-updating, relational database to coordinate and facilitate in silico modeling of Escherichia coli. *Nucleic Acids Res.* **32**, D293–D295 (2004).
32 S. G. Schultz, N. L. Wilson, W. Epstein, Cation transport in Escherichia coli. II. Intracellular chloride concentration. *J. Gen. Physiol.* **46**, 159–166 (1962).
33 P. Douzou, P. Maurel, Ionic control of biochemical reactions. *Trends Biochem. Sci.* **2**, 14–17 (1977).
34 H. Wennerström, Electrostatic interactions in concentrated colloidal dispersions. *Phys. Chem. Chem. Phys.* **19**, 23849–23853 (2017).
35 B. Derjaguin, Friction and adhesion. IV. The theory of adhesion of small particles. *Kolloid Zeits* **69**, 155–164 (1934).
36 G. Schreiber, A. R. Fersht, Energetics of protein-protein interactions: Analysis of the barnase-barstar interface by single mutations and double mutant cycles. *J. Mol. Biol.* **248**, 478–486 (1995).
37 S. Cayley, M. T. Record, Jr, Roles of cytoplasmic osmolytes, water, and crowding in the response of Escherichia coli to osmotic stress: Biophysical basis of osmoprotection by glycine betaine. *Biochemistry* **42**, 12596–12609 (2003).
38 C. M. Burgess *et al.*, The response of foodborne pathogens to osmotic and desiccation stresses in the food chain. *Int. J. Food Microbiol.* **221**, 37–53 (2016).
39 D. S. Cayley, H. J. Guttman, M. T. Record, Jr, Biophysical characterization of changes in amounts and activity of Escherichia coli cell and compartment water and turgor pressure in response to osmotic stress. *Biophys. J.* **78**, 1748–1764 (2000).
40 N. F. Carnahan, K. E. Starling, Equation of state for nonattracting rigid spheres. *J. Chem. Phys.* **51**, 635–636 (1969).
41 D. F. Evans, Self-organization of amphiphiles. *Langmuir* **4**, 3–12 (1988).
42 M. A. Gebbie, H. A. Dobbs, M. Valtiner, J. N. Israelachvili, Long-range electrostatic screening in ionic liquids. *Proc. Natl. Acad. Sci. U.S.A.* **112**, 7432–7437 (2015).
43 A. M. Smith, A. A. Lee, S. Perkin, The electrostatic screening length in concentrated electrolytes increases with concentration. *J. Phys. Chem. Lett.* **7**, 2157–2163 (2016).
44 M. A. Gebbie *et al.*, Long range electrostatic forces in ionic liquids. *Chem. Commun. (Camb.)* **53**, 1214–1224 (2017).
45 R. Kjellander, Decay behavior of screened electrostatic surface forces in ionic liquids: The vital role of non-local electrostatics. *Phys. Chem. Chem. Phys.* **18**, 18985–19000 (2016).
46 R. Kjellander, Focus article: Oscillatory and long-range monotonic exponential decays of electrostatic interactions in ionic liquids and other electrolytes: The significance of dielectric permittivity and renormalized charges. *J. Chem. Phys.* **148**, 193701 (2018).
47 A. A. Lee, C. S. Perez-Martinez, A. M. Smith, S. Perkin, Scaling analysis of the screening length in concentrated electrolytes. *Phys. Rev. Lett.* **119**, 026002 (2017).
48 A. H. Elcock, J. A. McCammon, Electrostatic contributions to the stability of halophilic proteins. *J. Mol. Biol.* **280**, 731–748 (1998).
49 H. X. Zhou, X. Pang, Electrostatic interactions in protein structure, folding, binding, and condensation. *Chem. Rev.* **118**, 1691–1741 (2018).
50 J. M. Wood *et al.*, Osmosensing and osmoregulatory compatible solute accumulation by bacteria. *Comp. Biochem. Physiol. A Mol. Integr. Physiol.* **130**, 437–460 (2001).
51 D. Bratko, A. Striolo, J. Z. Wu, H. W. Blanch, J. M. Prausnitz, Orientation-averaged pair potentials between dipolar proteins or colloids. *J. Phys. Chem. B* **106**, 2714–2720 (2002).
52 W. Li, B. A. Persson, M. Lund, J. Bergenholtz, M. Zackrisson Oskolkova, Concentration-induced association in a protein system caused by a highly directional patch attraction. *J. Phys. Chem. B* **120**, 8953–8959 (2016).
53 B. Jönsson, H. Wennerström, Image-charge forces in phospholipid bilayer systems. *J. Chem. Soc., Faraday Trans. 2* **79**, 19–35 (1983).
54 J. M. Wood, Bacterial responses to osmotic challenges. *J. Gen. Physiol.* **145**, 381–388 (2015).
55 A. M. Whatmore, R. H. Reed, Determination of turgor pressure in Bacillus subtilis: A possible role for K+ in turgor regulation. *J. Gen. Microbiol.* **136**, 2521–2526 (1990).
56 A. E. Walsby, The pressure relationships of halophilic and non-halophilic prokaryotic cells determined by using gas vesicles as pressure probes. *FEMS Microbiol. Rev.* **2**, 45–49 (1986).
57 A. Eiler *et al.*, Tuning fresh: Radiation through rewiring of central metabolism in streamlined bacteria. *ISME J.* **10**, 1902–1914 (2016).
58 K. L. Britton *et al.*, Analysis of protein solvent interactions in glucose dehydrogenase from the extreme halophile Haloferax mediterranei. *Proc. Natl. Acad. Sci. U.S.A.* **103**, 4846–4851 (2006).
59 G. Ortega, T. Diercks, O. Millet, Halophilic protein adaptation results from synergistic residue-ion interactions in the folded and unfolded states. *Chem. Biol.* **22**, 1597–1607 (2015).
60 J. A. Ranea, D. W. Buchan, J. M. Thornton, C. A. Orengo, Evolution of protein superfamilies and bacterial genome size. *J. Mol. Biol.* **336**, 871–887 (2004).
61 B. J. Tully, Metabolic diversity within the globally abundant Marine Group II Euryarchaea offers insight into ecological patterns. *Nat. Commun.* **10**, 271 (2019).
62 A. Oren, *Halophilic Microorganisms and their Environments* (Kluwer Academic Publishers, 2002), vol. 17, p. 3300.
63 C. M. Davis, M. Gruebele, S. Sukenik, How does solvation in the cell affect protein folding and binding? *Curr. Opin. Struct. Biol.* **48**, 23–29 (2018).
64 R. H. Vreeland, W. D. Rosenzweig, D. W. Powers, Isolation of a 250 million-year-old halotolerant bacterium from a primary salt crystal. *Nature* **407**, 897–900 (2000).